Ab initio vibrational predissociation dynamics of $He-I_2(B)$ complex

Álvaro Valdés, Rita Prosmiti,[a] Pablo Villarreal, and Gerardo Delgado-Barrio
Instituto de Matemáticas y Física Fundamental, CSIC, Serrano 123, 28006 Madrid, Spain

Didier Lemoine[b] and Bruno Lepetit[c]
Laboratoire Collisions, Agrégats, Réactivité (UMR 5589 CNRS-Université Paul Sabatier Toulouse 3), Institut de Recherche sur les Systèmes Atomiques et Moléculaires Complexes, 31062 Toulouse Cedex 9, France

(Received 17 April 2007; accepted 18 May 2007; published online 29 June 2007)

Three-dimensional quantum mechanical calculations on the vibrational predissociation dynamics of HeI_2 B state complex are performed using a potential energy surface accurately fitted to unrestricted open-shell coupled cluster *ab initio* data, further enabling extrapolation for large I_2 bond lengths. A Lanczos iterative method with an optimized complex absorbing potential is used to determine energies and lifetimes of the vibrationally predissociating $He,I_2(B,v')$ complex for $v' \leqslant 26$ of I_2 vibrational excitations. The calculated predissociating state energies agree with recent experimental results within 0.5 cm^{-1}. This excellent agreement is remarkable since no adjustment was made with respect to the experiments. The present *ab initio* approach, however, shows its limitations in the fact that the computed lifetimes that are highly sensitive to subtle details of the potential energy surfaces such as anisotropy, are a factor of 1.5 larger than the available experimental data. © *2007 American Institute of Physics*. [DOI: 10.1063/1.2748404]

I. INTRODUCTION

Extensive experimental and theoretical efforts have been made over the past three decades to understand the vibrational predissociation dynamics of triatomic rare gas-dihalogen systems.[1,2] The HeI_2 molecule was the first rare gas-dihalogen van der Waals (vdW) cluster that has been extensively studied by Levy *et al.*[3–8] The HeI_2 complex was first detected through laser induced excitation fluorescence spectra in which narrow bands were found to be shifted to the blue with respect to those of uncomplexed iodine.[3–5] Bands associated to ground and excited vdW modes have been observed.[3,6] Information on the geometry of the complex has been obtained by analyzing the rotational structure of the bands.[7] Lifetimes of the complex were estimated in the range of $I_2(v'=12-26)$ vibrational excitation[8] from the analysis of the spectral linewidths, and then extended up to $v'=68$.[9] Later, real-time studies[10] confirmed these results for a limited range of $v'=17-23$ levels. Iodine product state distributions have been also measured[6] as well as the binding energies of the complex in the ground X and excited B states.[4,5] In addition, Jahn *et al.* have reevaluated the ground-state binding energy of the HeI_2 molecule based on their experimental results on $HeBr_2$.[11] Recently, Ray *et al.*[12] have published a joint theoretical-experimental study of the $B \leftarrow X$ spectrum, which they interpret as resulting from the contribution of multiple (T-shaped and linear) conformers of $He-I_2$ complex. Furthermore, they have reported new estimates of the binding energies and structures of the ground and B excited state isomers.

Early theoretical studies were able to reproduce many of the experimental trends found for HeI_2 complex albeit using simple pairwise analytical potentials.[13–16] In particular, the energy gap law emerged as a powerful tool to interpret the variations of complex lifetimes with respect to iodine vibrational excitation. Recent comparisons between *ab initio* calculations and experimental data have shown that coupled cluster [CCSD(T)] methods provide potential energy surfaces (PESs), that reproduce theoretical data consistent with spectroscopic measurements.[17–22] The overall anisotropy predicted by such *ab initio* computations for rare gas-dihalogen systems is generally correct, although the resulting binding energies typically underestimate the experimental ones by 2–3 cm^{-1}.[23–25] Recent *ab initio* CCSD(T) studies of the PESs of the heavy HeI_2 complex for both its ground X and excited B electronic states[26,27] show that the anisotropy in this complex is qualitatively similar to that in the lighter, e.g., $HeCl_2$[18] and $HeBr_2$,[28,29] systems: whereas the ground state PES is characterized by two attractive wells about the linear and the perpendicular geometries, respectively, the B excited PES displays a single minimum about the T-shaped configuration. The $HeI_2(B)$ UCCSD(T) surface[27] has been also found reasonably consistent with different empirical potentials.[30,31]

In this paper, we use the above mentioned X and B *ab initio* PESs to calculate energies and lifetimes of the predissociating HeI_2 complex states,

$$HeI_2^*(B,v' \leqslant 26,n') \rightarrow He + I_2(B,v'_f < v'). \quad (1)$$

n' refers to the vdW excitation of the complex and v'_f to the final vibrational state of the iodine molecule. These calculations require the knowledge of the B PES in a range of I_2 internuclear distances larger than the ones provided by the *ab*

[a]Electronic mail: rita@imaff.cfmac.csic.es
[b]Electronic mail: didier.lemoine@irsamc.ups-tlse.fr
[c]Electronic mail: bruno.lepetit@irsamc.ups-tlse.fr

initio grid.[27] A new fitting procedure was developed to extrapolate the potential to large I_2 internuclear separations. This procedure is described in Sec. II. In Sec. III we present the Lanczos method used to compute energies and lifetimes for this potential. The results are compared with available experimental data which allows us to assess the quality of the present *ab initio* based PES. Finally, a summary and an outlook are given in Sec. IV.

II. POTENTIAL ENERGY SURFACES: REPRESENTATION OF *X* AND *B* STATES

The functional form and parameters from Ref. 26 are used for the *X* state potential. They represent the highest level *ab initio* potential available at present, and yield results consistent with the available experimental data.[32] The computed binding energies of the ground *T*-shaped and linear isomers are 14.7 and 15.4 cm^{-1}, respectively. These values are in good agreement with the early experimental estimates of 18.8 ± 0.6 cm^{-1} from Blazy *et al.*[5] and of 17.6 ± 1 cm^{-1} from Jahn *et al.*,[11] for the *T*-shaped isomer, as well as with the most recent experimental measurements reported by Ray *et al.*[12] of 16.6 ± 0.6 and 16.3 ± 0.6 cm^{-1} for *T*-shaped and linear isomers, respectively. As it can be seen the agreement has become very good with the latest experimental determinations. It is important to note that the ordering of the two isomers is reverse; however, their binding energies are very close to each other so that these should be both significantly populated when the HeI_2 complex is in its *X* state.

Recently, *ab initio* calculations[27] have been performed in order to represent the *B* state PES. The *B* potential has been built from a three-dimensional grid of *ab initio* points as a function of (R,r,θ), where *R* is the distance from He to the center of mass of I_2, *r* is the I_2 bond distance, and θ is the angle between **R** and **r**. The grid in *R* coordinate extends from 3 to 9 Å. There are seven values of θ between 0 and $\pi/2$. The grid in *r* consists of five values: 2.65, 2.85, 3.024, 3.20, and 3.45 Å, chosen around the equilibrium distance of the molecular iodine in its *B* excited electronic state. The PES has been generated from an interpolation procedure involving a Legendre expansion in θ, a fit to Morse-van der Waals functions in *R*, and a cubic-spline interpolation in *r* (see Ref. 27). In the present study, we need to consider vibrationally highly excited states of I_2 molecules, up to $v'=26$. However, the *r* range retained for the *ab initio* grid is not large enough to cover the v' values of interest. This is illustrated in Fig. 1 that shows the radial extension of a few vibrational states of I_2, including the $v'=26$. It has been shown[27] that achieving convergence with UCCSD(T) computations for larger *r* bond lengths is difficult. Thus, a reliable extrapolation scheme has to be introduced for large values of *r*. Here, a three-step procedure is employed for the representation of the *B* state potential. First, the UCCSD(T) *ab initio* data from Ref. 27 are fitted to a sum of Morse potentials, such as

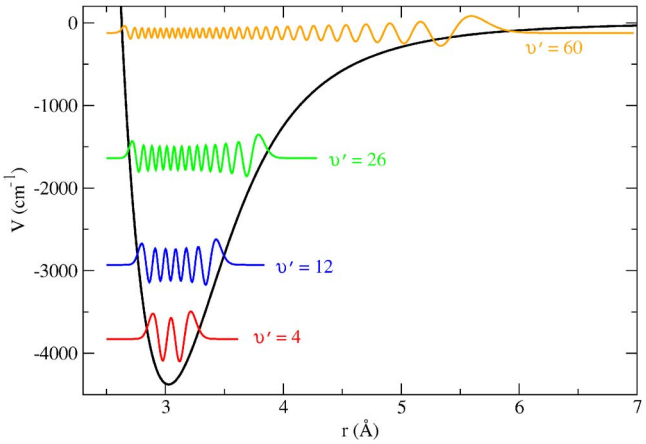

FIG. 1. (Color online) Selected vibrational wave functions of $I_2(B)$ superimposed on the diatomic potential energy curve. The corresponding energies are given in Table III, for up to $v'=26$.

$$V(R;r_k;\theta_l)=\sum_{j=1}^{2}\alpha_0^{lk}(\exp(-2\alpha_1^{lk}(x_j^l(R,r_k)-\alpha_2^{lk}))-2\exp(-\alpha_1^{lk}(x_j^l(R,r_k)-\alpha_2^{lk}))), \quad (2)$$

where $x_j^l(R,r_k)$ is the distance between He and each iodine atom indexed by $j=1$ or 2, namely,

$$x_j^l(R,r_k)=(R^2+(r_k/2)^2\pm Rr_k\cos\theta_l)^{1/2}, \quad (3)$$

where the $\pm$ sign refers to the $j=1,2$ selection. The values of the adjustable parameters α_0^{lk}, α_1^{lk}, and α_2^{lk} are obtained for the different θ_l and r_k, using a nonlinear least square fit. A mean standard deviation of the order of 0.3 cm^{-1} was obtained, with the maximum standard deviation being 0.39 cm^{-1} for $(r,\theta)=(3.024\text{ Å},30°)$.

Next, the α_0^{lk}, α_1^{lk}, and α_2^{lk} parameters are fitted to a function of *r* for each angle θ_l, which allows us to extrapolate to larger values of *r*, namely,

$$\alpha_i^l(r)=b_{0i}^l(1-\exp(-b_{1i}^l/r))^2+b_{2i}^l, \quad (4)$$

where $i=0$, 1, and 2. Table I reports the adjusted values of the b_0, b_1, and b_2 parameters, and Fig. 2 displays the $\alpha_0^l(r)$, $\alpha_1^l(r)$, and $\alpha_2^l(r)$ functions, plotted together with the values α_i^{lk}. It can be seen that the functional form [Eq. (4)] provides a good interpolation of the α_i^{lk} especially for $i=0$ and 2. We can thus expect a reasonable extrapolation behavior. The PES functional form now reads for each angular value

$$V(R,r;\theta_l)=\sum_{j=1}^{2}\alpha_0^l(r)(\exp(-2\alpha_1^l(r)(x_j(R,r)-\alpha_2^l(r)))-2\exp(-\alpha_1^l(r)(x_j(R,r)-\alpha_2^l(r)))). \quad (5)$$

The third step consists in a cubic-spline interpolation in the angle θ, which then yields the fully mapped PES.

This model potential represents the *ab initio* points accurately with an average error of 0.374 cm^{-1} and a maximum deviation of 3.4 cm^{-1} at $(R,r,\theta)=(4.5\text{ Å},3.2\text{ Å},45°)$ for which the potential value is $V=127.5$ cm^{-1}. Figure 3 displays the dependence on *R* for $\theta=90°$ and four distinct values of

TABLE I. Adjusted b_{mi}^{l} parameters from Eq. (4) with m, $i=0-2$ and $l=1-7$.

θ	b_0	b_1	b_2
		α_0	
0°	−0.00290209	−10.5836	20.4324
15°	−0.00164375	−11.1544	20.0427
30°	−3.29808E−06	−18.5225	18.4174
45°	−0.00702909	−8.01156	18.6254
60°	−2.45441 E−23	−67.1654	16.2107
75°	1.85837E−3	−8.85072	14.5415
90°	8.52615E−4	−10.9209	13.7193
		α_1	
0°	−4.93658E−13	−34.1552	1.4421
15°	−6.0554E−10	−24.7961	1.4421
30°	−1.9392E−19	−53.2176	1.4421
45°	−3.89506E−19	−51.6209	1.4421
60°	−0.00173119	−3.80448	1.4421
75°	1.43972E−07	−15.6365	1.4421
90°	2.54003E−07	−16.5116	1.4421
		α_2	
0°	0.000123003	−10.7481	4.04192
15°	3.13315E−05	−12.2487	4.0821
30°	4.00006E−07	−17.0634	4.15189
45°	0.00389734	−4.70609	4.14662
60°	−30914.3	−0.00348974	4.28178
75°	−8.0003E−4	−6.83454	4.31699
90°	−3.7465E−4	−8.3633	4.334

the r separation, which demonstrates the quality of the interpolation procedure upon comparison with the *ab initio* results, as well as the behavior of the extrapolation for the r value of 4.0 Å. Figure 4 shows the contour plot of the parametrized PES for the equilibrium I–I separation $r_e=3.024$ Å.[33] The new potential interpolation is very close to the one defined in Ref. 27. The T-shaped minimum is $D_e=29.65$ cm^{-1} for $R=3.973$ Å, to be compared with $D_e=29.48$ cm^{-1} for $R=3.96$ Å, for the potential of Ref. 27. The extrapolated PES was investigated in the region probed by the dynamical calculations and no unphysical behavior was detected.

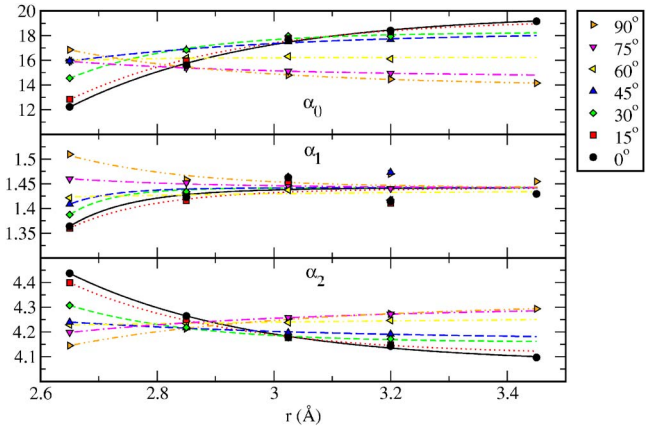

FIG. 2. (Color online) Dependence of the α_0, α_1, and α_2 parameters of Eq. (4) as a function of r and θ. The symbols refer to the *ab initio* results for each $\theta_{l=1-7}$ value (Ref. 27).

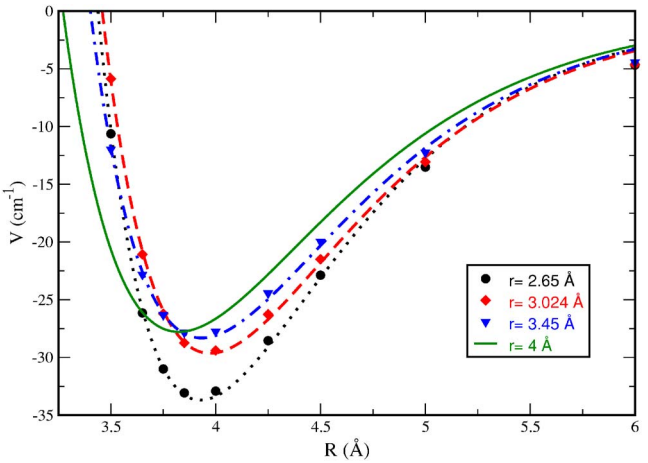

FIG. 3. (Color online) Analytical potential energy curves of T-shaped $HeI_2(B)$ for $r=2.65$ Å (dotted line), 3.024 Å (dashed line), 3.45 Å (dashed-dotted line), and 4.0 Å (solid line). The symbols refer to the *ab initio* results.

III. VIBRATIONAL PREDISSOCIATION

A. Method

The HeI_2 predissociating states are resonance states with lifetimes of the order of 100 ps.[8] As an alternative to time-dependent wave packet propagation methods[34,35] or to time-independent close coupling ones,[20,36,37] we compute the resonance states by diagonalizing the Hamiltonian of the system augmented by an imaginary potential in order to describe the coupling to the continuum.[38] The real and the imaginary parts of the complex eigenvalues, respectively, provide the energies and lifetimes of the resonance states.

We use a Lanczos iterative method to diagonalize the matrix. Detailed accounts of the method are given in Refs. 39–41. Basically, a tridiagonal matrix representation of the Hamiltonian is set up in a basis of Krylov vectors that are obtained through the successive application of the Hamiltonian on an initial random vector. The eigenvalues of the tridiagonal matrix yield the energy positions and widths (and hence the lifetimes) of the resonance states. The Lanczos approach is particularly well suited whenever one is seeking only a few low-lying states.

The numerical effort associated with each Lanczos itera-

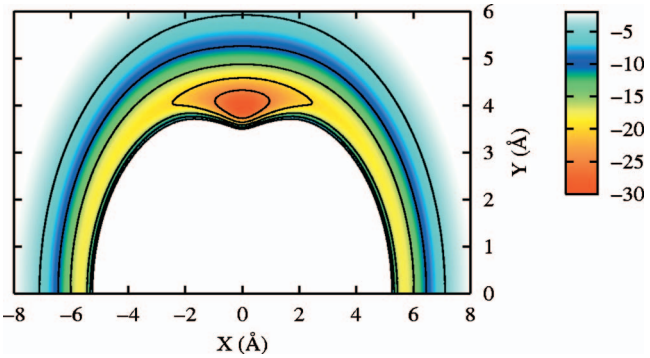

FIG. 4. (Color) Contour plot of the $HeI_2(B)$ potential, $V(R,r,\theta)$ [see Eq. (5)], in the (X,Y) plane. The I_2 molecule is aligned along X axis and He atom is moving in the (X,Y) plane. The I–I separation is fixed at its equilibrium value $r_e=3.024$ Å. Contour lines are for energies from −25 to 5 cm^{-1} by steps of 5 cm^{-1}.

TABLE II. Binding energies in cm^{-1} of the $He-I_2$ conformers in the indicated electronic and vibrational states.

Electronic state	I_2 level (v)	$He-I_2$ level (n)	Energy (conformer) Calc. value	Expt. value (Ref. 12)
$X\,^1\Sigma^+$	0	0	−15.4 (linear)[a]	−16.6 (T shaped)
	0	1,2	−14.7 (T shaped)[a]	−16.3 (linear)
$B\,^3\Pi_0^+$	19	0	−12.36 (T shaped)	−12.9 (T shaped)
	20	0	−12.35 (T shaped)	−12.8 (T shaped)
	21	0	−12.34 (T shaped)	−12.8 (T shaped)
	22	0	−12.34 (T shaped)	−12.8 (T shaped)
	23	0	−12.33 (T shaped)	−12.7 (T shaped)

[a]From Ref. 26.

tion can be much reduced owing to an efficient algorithm for the action of the Hamiltonian operator on the Krylov vectors. The Hamiltonian of the system can be written in Jacobi coordinates for a zero total angular momentum as

$$\hat{H} = T_R + H_r + T_\theta + W(R,r,\theta), \tag{6}$$

with

$$T_R = -\frac{\hbar^2}{2\mu_1}\frac{\partial^2}{\partial R^2}, \tag{7}$$

$$H_r = -\frac{\hbar^2}{2\mu_2}\frac{\partial^2}{\partial r^2} + V_{I_2}(r), \tag{8}$$

and

$$T_\theta = -\left(\frac{\hbar^2}{2\mu_1 R^2} + \frac{\hbar^2}{2\mu_2 r^2}\right)\frac{1}{\sin\theta}\frac{\partial}{\partial\theta}\sin\theta\frac{\partial}{\partial\theta}, \tag{9}$$

$$W(R,r,\theta) = V(R,r,\theta) - V_{I_2}(r). \tag{10}$$

$V(R,r,\theta)$ is the electronic potential of the system described in Sec. II [see Eq. (5)], augmented by the complex absorbing potential. $V_{I_2}(r)$ is the potential of the isolated I_2 molecule.[42] The reduced masses are given by $1/\mu_1 = 1/m_{He} + 1/2m_I$ and $1/\mu_2 = 1/m_I + 1/m_I$ (we use $m_{He} = 4.002\,60$ and $m_I = 126.90\,447$ amu). The wave function is defined by its expansion coefficients C_{vnj} in a direct product basis as

$$\psi(R,r,\theta) = \sum_{vnj} C_{vnj}\chi_v(r)g_n(R)P_j(\cos\theta), \tag{11}$$

where $\chi_v(r)$, v in the range $[v_{min}, v_{max}]$, are the vibrational eigenfunctions of the nonrotating diatomic $I_2(B)$. The $g_n(R)$, $n \leqslant n_{max}$, are sine waves $\sin[k_n(R-R_{min})]$, with $k_n = 2\pi n/(R_{max}-R_{min})$, and $P_j(\cos\theta)$, $j \leqslant j_{max}$, are Legendre polynomials. Calculation is performed in the box $[R_{min}, R_{max}]\times[r_{min}, r_{max}]\times[0,\pi]$. Since the two iodine atoms are identical we only keep even or odd values of j according to the symmetry to be studied. Since $\chi_v(r)$, $g_n(R)$, and $P_j(\cos\theta)$ are eigenfunctions of the operators H_r, T_R, and T_θ, respectively, the action of these operators on the direct products of Eq. (11) is straightforward. Computing the action of $W(R,r,\theta)$ on the expansion of Eq. (11) requires the evaluation of the basis functions on a grid of $N_R \times N_r \times N_\theta$ points by transformation methods. A fast sine transform[43,44] is applied along R, a symmetrized Legendre transformation[45] is used along θ, and a potential optimized (PO) transformation is defined by diagonalizing the r operator[46,47] in the $\chi_v(r)$ vibrational basis.

An optimized cubic absorbing potential[48] V_{opt} is used for $R \geqslant R_{opt}$,

$$V_{opt} = \begin{cases} 0, & R_{min} \leqslant R \leqslant R_{opt} \\ -i\eta((R-R_{min})/(R_{max}-R_{min}))^3, & R_{opt} \leqslant R \leqslant R_{max}. \end{cases}$$

Convergence studies led to the following choice of parameters. For the angular coordinate we used $N_\theta = 53$ quadrature points and $j_{max} = 20$, corresponding to 10 or 11 Legendre polynomials depending on the symmetry. In the r coordinate $N_r = 28$ PO quadrature points are used in the interval $[r_{min}, r_{max}] = [2.65-3.92]$ Å and ten vibrational basis functions $\chi_v(r)$ are used in the range $[v'-4-v'+5]$ where v' is the vibrational excitation of the targeted resonance. In the R coordinate $N_R = 61$ grid points are used in the interval $[R_{min}, R_{max}] = [2.5-17.5]$ Å, contracted to 48 g_n functions by discarding plane waves with energies larger than 410 cm^{-1}.

The cubic absorbing potential was designed with respect to a relative semiclassical error[48] less than 10^{-8} for a maximum dissociation energy of 121 cm^{-1}. This is roughly the kinetic energy of the fragments at large separation since it is known that for an initially excited $HeI_2(v')$ complex most of the products are in the state $I_2(v'-1)$, so that the kinetic energy available is roughly one quantum of vibration of the iodine molecule, at least in the range of v' values studied here. This choice leads to $R_{opt} = 9.5$ Å and $\eta = 247$ cm^{-1}.

The sought energy values and the lifetimes are converged within 4000 Lanczos iterations. The absolute accuracy of the results is estimated to be of the order of 0.01 cm^{-1} for the energies and as good as 1 ps for the lifetimes.

B. Lifetimes and blueshifts

Table II reports the comparison of computed binding energies for the $He-I_2$ conformers, in both X and B states, in comparison with the experimental measurements from Ref. 12. The calculated values pertaining to $v' = 19-23$ in Table II were obtained with the extrapolated B surface. As it can be

TABLE III. Experimental and calculated spectral blueshifts for the $HeI_2(B,v') \leftarrow (X,v=0)$ transition between the *T*-shaped vdW ground levels. The value $D_0^T(X,v'=0)=14.68$ cm^{-1} of Ref. 26 is used in fourth column. Columns 2 and 3 refer to the energies of $I_2(B,v',j'=0)$ and to the dissociation energies of $HeI_2(B,v',n'=0)$, respectively. All energies are in cm^{-1}.

			Blueshift	
v'	$E_{I_2(B)}^{v',j'=0}$	$E_{HeI_2(B)}^{v',j=0,n'=0}$	This work	Expt. (Refs. 3–5)
0	0.0	−12.51	2.17	⋯
1	123.58	−12.50	2.18	⋯
2	246.28	−12.50	2.18	⋯
3	367.59	−12.49	2.19	3.44
4	487.33	−12.49	2.19	3.44
5	605.35	−12.48	2.20	3.46
6	721.65	−12.48	2.20	3.49
7	836.28	−12.47	2.21	3.46
8	949.27	−12.46	2.22	3.51
9	1060.62	−12.45	2.23	3.60
10	1170.31	−12.45	2.23	3.58
11	1278.29	−12.44	2.24	3.62
12	1384.53	−12.43	2.25	3.69
13	1488.97	−12.42	2.26	3.60
14	1591.61	−12.41	2.27	3.68
15	1692.44	−12.40	2.28	3.66
16	1791.44	−12.39	2.29	3.70
17	1888.60	−12.38	2.30	3.73
18	1983.90	−12.37	2.31	3.73
19	2077.30	−12.36	2.32	3.75/3.7[a]
20	2168.78	−12.35	2.33	3.76/3.8[a]
21	2258.30	−12.34	2.34	3.8/3.8[a] /3.79[b]
22	2345.86	−12.34	2.35	3.81/3.8[a]
23	2431.43	−12.33	2.35	3.86/3.9[a]
24	2515.03	−12.33	2.36	3.87
25	2596.63	−12.32	2.36	3.9
26	2676.30	−12.32	2.36	3.91

[a]From Ref. 12.
[b]From Ref. 10.

seen, the resulting $He+I_2(B,v')$ vdW energies for the *T*-shaped isomers are in excellent agreement with the recent experimental data reported by Ray *et al.*,[12] e.g., for $v'=20$ a computed value of 12.35 cm^{-1} is obtained, that is within the experimental measurement of 12.8 ± 0.6 cm^{-1}.

The first experimental measurements available on HeI_2 were the blueshifts with respect to the uncomplexed iodine bands.[3] The blueshifts correspond to the difference between the dissociation energies of the initial and final states of the transition, namely, $D_0^T(B,v',n')$-$D_0^T(X,v=0)$ or $D_0^T(B,v',n')$-$D_0^L(X,v=0)$, according to the initial *T*-shaped or linear isomer in its ground vdW state. The first feature shifted nearly 4 cm^{-1} to higher energies in the experiments by Ray *et al.*[12] can be attributed to the transition between the initial *T*-shaped state of $HeI_2(X,v=0)$ and the excited complex $HeI_2(B,v',n'=0)$ in its ground vdW state. The computed blueshifts based on *T*-shaped binding energies are reported in Table III for a wide range of v' values, and compared with earlier experimental data by Levy and co-workers,[3–5] as well as with the recent experimental estimates by Ray *et al.*,[12] in the range of $v'=19-23$. The calculated results are systematically lower than the measured ones by 1.2–1.6 cm^{-1}. This discrepancy reflects the fact that the computed *T*-shaped dissociation energies are underestimated by roughly 2 cm^{-1} for the *X* state and by about 0.5 cm^{-1} for the *B* state (see Table II).

TABLE IV. Experimental and theoretical energies in cm^{-1} for the $He+I_2(B,v'=20)$ vdW levels. The value $D_0^L(X,v'=0)=15.38$ cm^{-1} of Ref. 26 is used to calculate the expected spectral blueshifts arising from the linear isomer in the fifth column.

	$E_{HeI_2(B,v'=20,n')}$		Blueshift	
n'	Expt. (Ref. 12)	This work	Expt. (Ref. 12)	This work
0	−12.8	−12.35	3.8	3.03
1	⋯	−8.27	⋯	7.11
2	−7.9	−7.64	8.7/9.67[a]	7.74
3	−6.8	−6.83	9.8	8.55
4	−5.7	−5.86	10.9	9.52
5	−4.2	−4.24	12.4	11.14
6	−2.2	−2.57	14.4	12.81

[a]From Ref. 3.

Blueshifts were also measured for the first excited band, which corresponds to the *C* band in the early work of Smalley *et al.*[3] This band has been attributed[3,12] to the contribution of vdW excited modes $n' \geqslant 2$ for the *B* state. In order to analyze their recent experimental data, Ray *et al.*[12] have relied on a semiempirical pairwise-additive *B*-state potential that also displays a single well about the *T*-shaped configuration. Using an adiabatic description of the I_2 vibrational motion, they have computed the associated vdW states. The ground $(n'=0)$ state and the first excited $(n'=1)$ one are found localized in the *T*-shaped well, whereas the higher excited $(n'=2-6)$ states are delocalized (free-rotorlike) and have their largest amplitude for near-linear configurations. As a result, these highly excited states have significant overlaps only with the linear *X* isomer. Because the $n'=1$ state remains localized about the *T*-shaped configuration it could provide an experimentally detectable band only for excitation from the *T*-shaped isomer, if the latter was not forbidden by symmetry. Hence, only bands corresponding to $n'>1$ can be detected. Our *B*-state potential induces the same kind of distribution of vdW states as can be seen in Fig. 3 of Ref. 32. Thus, we can assess blueshifts for the excited band based on the $n'=2-6$ series of the *B* state.

Our computed blueshifts, namely, $D_0(B,v'=20,n')$-$D_0^L(X,v=0)$, are reported in Table IV for $n'=0-6$, and for the vibrational manifold $v'=20$ specifically investigated by Ray *et al.*[12] The values given by Smalley *et al.*[3] lie between 9.46 and 9.88 cm^{-1} in the v' range 9–29. However, the so-called *C* band is broad and multimodal so that it is not entirely clear to which feature the values refer. Yet, Ray *et al.* provide in their Fig. 7(a) an enlargement of the excited band spectrum that was recorded between roughly 8.5 and 14 cm^{-1}, away from the I_2 band origin. Four main maxima can be seen in this range. The first peak is located at 9.3–9.4 cm^{-1}, thus corresponding closely to the value of 9.67 cm^{-1} of Smalley *et al.* for $v'=20$. The computed blueshifts extend from 7.74 cm^{-1} for $n'=2$ to 12.81 cm^{-1} for $n'=6$. We have pointed out the systematic departure from

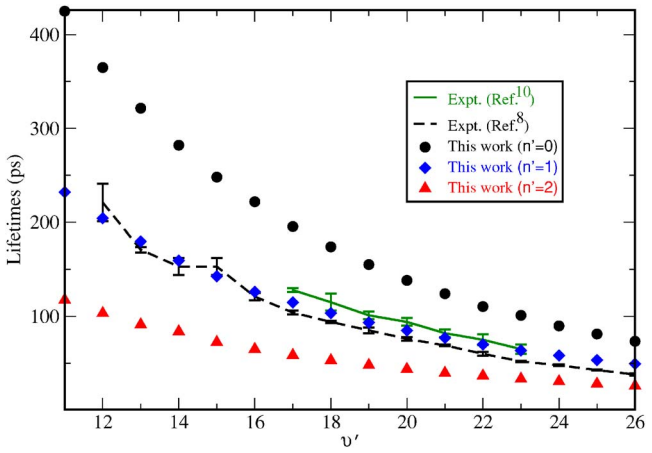

FIG. 5. (Color online) Experimental [solid (Ref. 10) and dashed (Refs. 8 and 9) lines] and theoretical (symbols) lifetimes for the vibrational predissociation of $HeI_2(B)$ as a function of the $I_2(B)$ vibrational excitation. The calculated lifetimes are shown for vdW modes $n'=0$ (circles), 1 (diamonds), and 2 (triangles).

TABLE V. Experimental and calculated vibrational predissociation lifetimes in picosecond for $HeI_2(B,v',n'=0)$.

v'	This work	Expt. (Ref. 8)	Expt. (Ref. 10)
12	364.9	221±20	···
13	321.5	171±3	···
14	282.1	153±9	···
15	248.1	153±9	···
16	221.8	121±4	···
17	195.4	104±2	128±2
18	174	94±1	115±9
19	155.1	85±3	101±4
20	138.3	76±2	94±4
21	124.1	69±1	82±4
22	110.4	60±2	75±6
23	101	51.9±0.7	65±5
24	89.78	47.7±0.9	···
25	81.13	42.7±0.5	···
26	73.29	37.9±1.3	···

experimental measurements in the case of the blueshift calculated for the ground $n'=0$ state, mainly because of a slightly inaccurate determination of the X state dissociation energy. As will be discussed hereafter, the error made on the positions of the excited vdW levels in the upper B state is quite small. The computed dissociation energy for the X-state linear isomer is smaller by roughly 1 cm^{-1} with respect to experiment (see Table II). Shifting the computed blueshifts by the same amount results in a perfect match with the experimental spectral range of the excited band depicted in the upper curve of the left panel of Fig. 7(a) of Ray *et al.*[12] Finally, the fact that the intensity of the first peak of this curve is quite low can be easily understood if it corresponds to the contribution from the $n'=2$ state. Indeed, the overlap between the lesser delocalized $n'=2$ state and the ground linear isomer state may be quite weak in comparison to that involving the higher excited, free rotorlike states.

Table IV reports the computed binding energies of the B-state vdW levels for $v'=20$ and $n'=0-6$, as well as the values stemming from Table III of Ray *et al.*[12] Our calculations are in excellent agreement with the experimental determinations. For $n'=0$ the difference of 0.45 cm^{-1} is within the experimental uncertainty of 0.6 cm^{-1}. The agreement is even better for the excited states. The agreement is remarkable considering that our calculations are based upon an accurate fit of a purely *ab initio* PES and its extrapolation for larger r values, without any adjustment with respect to experimental data.

Measurements of lifetimes are also available for the ground states of the $HeI_2(B,v')$ complex.[8–10] In our calculations lifetimes are obtained from the imaginary part of the complex eigenvalues of the Hamiltonian. Their comparison with data from different experiments is shown in Fig. 5 and Table V. It is striking to note that computational results give the same trend as the experimental ones. There is, however, an almost constant factor of 1.5 between both sets of results. The decrease of the lifetime with excitation v' is a manifestation of the well known energy gap law, which breaks down at larger v' near 50–60 when the $v'-1$ channel closes. Again, the agreement between calculations and experiments can be considered as satisfactory, keeping in mind that slight modifications of the potential may change the lifetime dramatically.

Figure 5 shows the lifetimes obtained for the $HeI_2(B,v',n')$ complex with vdW excitations $n'=1$ and 2 in addition to those for the ground $n'=0$ state. It is seen that lifetimes gradually decrease as excitation increases. This is a direct consequence of the angular delocalization of excited states. The complex can then be found about the collinear configuration for which energy transfer from I_2 vibration to vdW mode is much more efficient.[49]

IV. CONCLUSIONS

The present study reports the first three-dimensional, fully quantum computation of the dynamical properties of the $HeI_2(B)$ excited vdW complex, based on a potential energy surface generated from an accurate fit to a set of calculated points obtained through a high-level *ab initio* theory, further enabling extrapolation for larger r values. The vibrational predissociation lifetimes and energies of $HeI_2(B,v')$ were characterized for the vibrational quantum numbers up to $v'=26$ of the $I_2(B)$ stretch and for the vdW excitation states $n'=0-6$. Energy positions and lifetimes of the complex were calculated using a complex symmetric Lanczos scheme incorporating an absorbing potential.

Our *ab initio* study provides energies for the B-state vdW levels in excellent agreement with the experimental ones, the discrepancy being at most 0.5 cm^{-1}, lower than the experimental uncertainty. The agreement is remarkable since no adjustment was made on the potential surfaces with respect to the experiments. Regarding lifetimes, the overall decrease for the ground vdW mode $n'=0$ as a function of I_2 vibrational excitation is well reproduced. There is, however, an almost constant factor of 1.5 between the computed and the measured lifetimes.

The next step following the present study would be to compute the complete absorption spectrum for both linear and T-shaped X state isomers.[19,21] Thereby, one could check

whether the $n'=0$ and $n'>0$ bands are entirely due to the *T*-shaped and linear isomers, respectively. A further step could be to obtain a fully *ab initio* surface for the *B* state, covering larger *r* values, as well as a refinement in order to improve the description of the *X* state potential. For such calculations more sophisticated multireference methods, such as multi-reference correlation interaction (MRCI), should be employed.

ACKNOWLEDGMENTS

The authors are grateful to Alberto Beswick and Timur Tscherbul for useful discussions. The Centro de Calculo (IMAFF), CTI (CSIC), CESGA, and MareNostrum (BSC) are acknowledged for allocation of computer time. One of the authors (A.V.) would like to thank CICYT, Spain for a grant to support his stay at the Laboratoire Collisions, Agrégats, Réactivité. One of the authors (R.P.) acknowledges support by Ramón y Cajal Programme Grant No. PDRYC-2006-001017. This work has been supported by DGICYT, Spain, Grant No. FIS2004-02461 and CSIC-CNRS, Grant No. 2005-FR0031.

[1] A. Rohrbacher, J. Williams, and K. C. Janda, Phys. Chem. Chem. Phys. **1**, 5263 (1999).
[2] A. Rohrbacher, N. Halberstadt, and K. C. Janda, Annu. Rev. Phys. Chem. **51**, 405 (2000).
[3] R. F. Smalley, D. H. Levy, and L. Wharton, J. Chem. Phys. **64**, 3266 (1976).
[4] J. E. Kenny, K. E. Johnson, W. Sharfin, and D. H. Levy, J. Chem. Phys. **72**, 1109 (1980).
[5] J. A. Blazy, B. M. DeKoven, T. D. Russell, and D. H. Levy, J. Chem. Phys. **72**, 2439 (1980).
[6] W. Sharfin, K. E. Johnson, L. Wharton, and D. H. Levy, J. Chem. Phys. **71**, 1292 (1979).
[7] R. F. Smalley, L. Wharton, and D. H. Levy, J. Chem. Phys. **68**, 671 (1978).
[8] K. E. Johnson, L. Wharton, and D. H. Levy, J. Chem. Phys. **69**, 2719 (1978).
[9] W. Sharfin, P. Kroger, and S. C. Wallace, Chem. Phys. Lett. **85**, 81 (1982).
[10] M. Gutmann, D. M. Willberg, and A. H. Zewail, J. Chem. Phys. **97**, 8037 (1992).
[11] D. G. Jahn, S. G. Clement, and K. C. Janda, J. Chem. Phys. **101**, 283 (1994).
[12] S. E. Ray, A. B. McCoy, J. J. Glennon, J. P. Darr, E. J. Fesser, J. R. Lancaster, and R. A. Loomis, J. Chem. Phys. **125**, 164314 (2006).
[13] J. A. Beswick and J. Jortner, Chem. Phys. Lett. **49**, 13 (1977).
[14] J. A. Beswick and J. Jortner, J. Chem. Phys. **68**, 2277 (1978).
[15] J. A. Beswick, G. Delgado-Barrio, and J. Jortner, J. Chem. Phys. **70**, 3895 (1979).
[16] J. A. Beswick and G. Delgado-Barrio, J. Chem. Phys. **73**, 3653 (1980).
[17] K. Higgins, F. M. Tao, and W. Klemperer, J. Chem. Phys. **109**, 3048 (1998).
[18] J. Williams, A. Rohrbacher, J. Seong, N. Marianayagam, K. C. Janda, R. Burcl, M. N. Szcześniak, G. Chalasiński, S. M. Cybulski, and N. Halberstadt, J. Chem. Phys. **111**, 997 (1999).
[19] A. A. Buchachenko, R. Prosmiti, C. Cuhna, P. Villarreal, and G. Delgado-Barrio, J. Chem. Phys. **117**, 6117 (2002).
[20] R. Prosmiti, C. Cunha, A. Buchachenko, G. Delgado-Barrio, and P. Villarreal, J. Chem. Phys. **117**, 10019 (2002).
[21] M. I. Hernández, T. González-Lezana, A. A. Buchachenko, R. Prosmiti, M. P. de Lara-Castells, G. Delgado-Barrio, and P. Villarreal, Recent Res. Devel. Chem. Physics **4**, 1 (2003).
[22] A. B. McCoy, J. P. Darr, D. S. Boucher, P. R. Winter, M. D. Bradke, and R. A. Loomis, J. Chem. Phys. **120**, 2677 (2004).
[23] R. Prosmiti, C. Cunha, G. Delgado-Barrio, and P. Villarreal, J. Chem. Phys. **117**, 7017 (2002).
[24] R. Prosmiti, C. Cunha, P. Villarreal, and G. Delgado-Barrio, J. Chem. Phys. **119**, 4216 (2003).
[25] A. Valdés, R. Prosmiti, P. Villarreal, and G. Delgado-Barrio, Chem. Phys. Lett. **357**, 328 (2003).
[26] R. Prosmiti, Á. Valdés, P. Villarreal, and G. Delgado-Barrio, J. Phys. Chem. A **108**, 6065 (2004).
[27] Á. Valdés, R. Prosmiti, P. Villarreal, G. Delgado-Barrio, and J-H. Werner, J. Chem. Phys. **126**, 204301 (2007).
[28] Á. Valdés, R. Prosmiti, P. Villarreal, and G. Delgado-Barrio, Mol. Phys. **102**, 2277 (2004).
[29] M. P. de Lara-Castells, A. A. Buchachenko, G. Delgado-Barrio, and P. Villarreal, J. Chem. Phys. **120**, 2182 (2004).
[30] S. K. Gray and C. E. Wozny, J. Chem. Phys. **94**, 2817 (1991).
[31] A. Garcia-Vela, J. Chem. Phys. **123**, 124311 (2005).
[32] G. Delgado-Barrio, R. Prosmiti, Á. Valdés, and P. Villarreal, Phys. Scr. **73**, C57 (2006).
[33] K. P. Huber and G. Herzberg, *Molecular Spectra and Molecular Structure IV. Constants of Diatomic Molecules* (Van Nostrand, Princeton, 1979).
[34] B. Lepetit, O. Roncero, A. A. Buchachenko, and N. Halberstadt, J. Chem. Phys. **116**, 8367 (2002).
[35] O. Roncero, A. A. Buchachenko, and B. Lepetit, J. Chem. Phys. **122**, 034303 (2005).
[36] O. Roncero, J. A. Beswick, N. Halberstadt, P. Villarreal, and G. Delgado-Barrio, J. Chem. Phys. **92**, 3348 (1990).
[37] F. X. Gadéa, H. Berriche, O. Roncero, P. Villarreal, and G. Delgado-Barrio, J. Chem. Phys. **107**, 10515 (1997).
[38] G. Jolicard and E. J. Austin, Chem. Phys. Lett. **121**, 106 (1985).
[39] J. K. Cullum and R. A. Willoughby, *Lanczos Algorithms for Large Symmetric Eigenvalue Computations* (SIAM, Philadelphia, 2002).
[40] *Templates for the Solution of Algebraic Eigenvalue Problems: A Practical Guide*, edited by Z. Bai, J. W. Demmel, J. J. Dongarra, A. Ruhe, and H. A. van der Vorst (SIAM, Philadelphia, 2000).
[41] F. Wippel, D. Lemoine, B. Lepetit, J. Kerwin, X. Sha, and B. Jackson (unpublished).
[42] S. Gerstenkorn and P. Luc, J. Phys. (France) **46**, 865 (1985).
[43] W. H. Press, S. A. Teukolsky, W. T. Vetterling, and B. P. Flannery, in *Numerical recipes: The Art of Scientific Computing*,2nd ed. (Cambridge University, Cambridge, 1992).
[44] A. Besprozvannaya and D. J. Tannor, Comput. Phys. Commun. **63**, 569 (1991).
[45] J. V. Lill, G. A. Parker, and J. C. Light, J. Chem. Phys. **85**, 900 (1986).
[46] J. Echave and D. C. Clary, Chem. Phys. Lett. **190**, 225 (1992).
[47] H. Wei and T. Carrington, J. Chem. Phys. **97**, 3029 (1992).
[48] U. V. Riss and H.-D. Meyer, J. Chem. Phys. **105**, 1409 (1996).
[49] O. Roncero, B. Lepetit, J. A. Beswick, N. Halberstadt, and A. A. Buchachenko, J. Chem. Phys. **115**, 6961 (2001).